A Multipopulation Multiobjective Ant Colony System Considering Travel and Prevention Costs for Vehicle Routing in COVID-19-Like Epidemics

Jian-Yu Li, *Student Member, IEEE*, Xin-Yi Deng, Zhi-Hui Zhan, *Senior Member, IEEE*, Liang Yu, Kay Chen Tan, *Fellow, IEEE*, Kuei-Kuei Lai, and Jun Zhang, *Fellow, IEEE*

***Abstract*— As transportation system plays a vastly important role in combatting newly-emerging and severe epidemics like the coronavirus disease 2019 (COVID-19), the vehicle routing problem (VRP) in epidemics has become an emerging topic that has attracted increasing attention worldwide. However, most existing VRP models are not suitable for epidemic situations, because they do not consider the prevention cost caused by issues such as viral tests and quarantine during the traveling. Therefore, this paper proposes a multi-objective VRP model for epidemic situations, named VRP4E, which considers not only the traditional travel cost but also the prevention cost of the VRP in epidemic situations. To efficiently solve the VRP4E, this paper further proposes a novel algorithm named multi-objective ant colony system algorithm for epidemic situations, termed MOACS4E, together with three novel designs. First, by extending the efficient "multiple populations for multiple objectives" framework, the MOACS4E adopts two ant colonies to optimize the travel and prevention costs respectively, so as to improve the search efficiency. Second, a pheromone fusion-based solution generation method is proposed to fuse the pheromones from different colonies to increase solution diversity effectively. Third, a solution quality improvement method is further proposed to improve the solutions for the prevention cost objective. The effectiveness of the MOACS4E is verified in experiments on 25 generated benchmarks by comparison with six state-of-the-art and modern algorithms. Moreover, the VRP4E in different epidemic situations and a real-world case in the Beijing-Tianjin-Hebei region, China, are further studied to provide helpful insights for combatting COVID-19-like epidemics.**

***Index Terms*— COVID-19, epidemics, vehicle routing problem, multi-objective optimization, evolutionary computation, ant colony system, multiple populations for multiple objectives.**

I. Introduction

SEVERE epidemics that may outbreak worldwide pose great threats to human beings and real-world society. For example, the coronavirus disease 2019 (COVID-19), a fast-spread respiratory disease, has caused more than five hundred million confirmed infections and over six million deaths worldwide from December 2019 to May 2022 [1], [2]. Moreover, although the vaccines have been started, the virus that causes COVID-19 mutates rapidly against the vaccines and related treatments. Therefore, it is predicted that the significant damage to society due to the COVID-19 epidemics will continue [3]–[5]. Under such a situation, people in various fields are jointly devoting efforts to combat the epidemics and save lives. In combatting COVID-19-like severe epidemics, transportation systems that can support daily operations in epidemic areas play a vastly important role [6]–[8]. However, transportation systems in epidemic situations have to face many great challenges, such as strict traffic control in epidemic areas, the infection among drivers and passengers, and the virus transmission via transportation networks. Therefore, the research on intelligent transportation systems that can address the challenges brought by serious epidemics is of great need and has become an emerging research topic.

In transportation systems, vehicle routing is one of the most essential and significant parts [9]. Therefore, this paper focuses on the vehicle routing problem (VRP) under epidemic conditions. Generally speaking, the basic goal of VRP is to obtain a vehicle route that serves all customers with a minimal travel cost [10], [11]. For different specific applications, various objectives and constraints can be added to form various VRP variants. For example, considering the capacity of the vehicle, the VRP can be easily transformed into the capacity VRP (CVRP), which is one of the most widely-studied VRP variants [12], [13]. Moreover, considering the objective such as waiting and delay time [14], environmental pollution [15], and energy consumption [16], various VRP models can be developed and researched. Therefore, the VRP and its variants, being NP-hard combination problems, have been widely studied and

Manuscript received 23 November 2021; revised 29 March 2022 and 24 May 2022; accepted 26 May 2022. Date of publication 17 June 2022; date of current version 5 December 2022. This work was supported in part by the National Key Research and Development Program of China under Grant 2019YFB2102100, in part by the National Natural Science Foundations of China under Grant 62176094 and Grant 61873097, in part by the Key-Area Research and Development of Guangdong Province under Grant 2020B010166002, and in part by the Guangdong Natural Science Foundation Research Team under Grant 2018B030312003. The Associate Editor for this article was Y.-J. Zheng. *(Corresponding authors: Zhi-Hui Zhan; Jun Zhang.)*

Jian-Yu Li and Zhi-Hui Zhan are with the School of Computer Science and Engineering, South China University of Technology, Guangzhou 510006, China, also with the Pazhou Laboratory, Guangzhou 510330, China, and also with the Guangdong Provincial Key Laboratory of Computational Intelligence and Cyberspace Information, Guangzhou 510006, China (e-mail: zhanapollo@163.com).

Xin-Yi Deng is with the School of Chinese Language and Literature, South China Normal University, Guangzhou 510631, China.

Liang Yu is with Alibaba, Feitian Campus, Hangzhou 330000, China.

Kay Chen Tan is with the Department of Computing, The Hong Kong Polytechnic University, Hong Kong.

Kuei-Kuei Lai is with the Department of Business Administration, Chaoyang University of Technology, Taichung 413, Taiwan.

Jun Zhang is with Hanyang University, Ansan 15588, South Korea.

This article has supplementary downloadable material available at https://doi.org/10.1109/TITS.2022.3180760, provided by the authors.

Digital Object Identifier 10.1109/TITS.2022.3180760

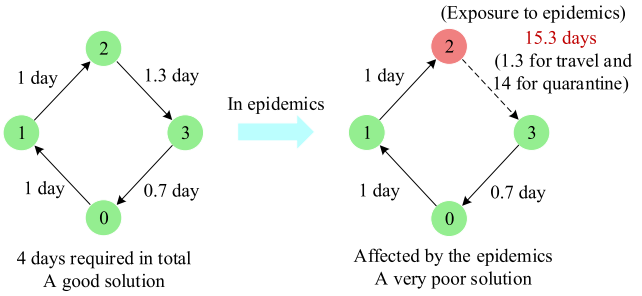

Fig. 1. The effects of epidemics on the quality of a routing solution.

applied in many real-world application areas and attracted wide attention from both academic research and industrial communities.

Although many VRP variants have been proposed and studied, they do not consider the influence of epidemics and thus are not suitable for epidemic situations, resulting in the gap between research and practice in combatting epidemics. Motivated by this, this paper attempts to explore the VRP that is suitable for epidemic situations. In particular, a major difference between VRP in the ordinary and epidemic situations is that various prevention and protection approaches have to be conducted to control the virus spread in epidemic scenarios, such as viral and antibody tests within 3 or 7 days, quarantine, self-isolation, and disinfecting of the products and vehicles [17]. As these prevention approaches will cost considerable time and money of drivers/customers and even stop their journey due to area lockdown and travel restrictions, the prevention cost becomes an important factor for the quality of a routing plan. For example, Fig. 1 shows that a good routing solution for ordinary situations can be very poor in the epidemic situation due to the quarantine. That is, a routing solution with the smallest travel distance may not have the smallest cost for prevention, and vice versa. Hence, this paper considers not only the travel cost objective but also the prevention cost objective of the VRP in epidemic situations, and then formulates a multi-objective VRP model for epidemics, which is named VRP4E. The reason for using multi-objective optimization is that the travel cost and the prevention cost objectives conflict with each other. Moreover, multi-objective optimization can provide a set of solutions for users to choose according to their preferences and requirements.

To solve the proposed challenging multi-objective combinational VRP4E problem, a suitable and efficient optimizer should be designed. As a well-known and widely-used evolutionary computation approach [18]–[21], ant colony optimization (ACO) [22], [23] has shown great efficiency in solving combinational optimization problems, such as autonomous robotics [24], cloud computing [25], and water system design [26]. In particular, the ant colony system (ACS) [22], as an efficient ACO variant, has been applied to various applications including VRP successfully in the past decade [27]–[29]. Therefore, this paper attempts to propose a better ACS variant for solving the VRP4E efficiently. As ACS is originally a single-objective algorithm, it should be integrated with multi-objective optimization techniques when solving the proposed multi-objective VRP4E problem. In recent years, a novel multiple populations for multiple objectives (MPMO) framework [33] has been proposed for multi-objective optimization. In the MPMO, multiple populations are co-evolved for solving the problem, where each population aims at one objective while all the populations cooperate to search the whole Pareto front. Due to its great efficiency and effectiveness, MPMO has been widely studied and has attracted increasing attention as a new multi-objective optimization framework in recent years [34]–[36]. Therefore, the ACS and the MPMO framework can be adopted as the basic component of a novel and efficient ACS algorithm to handle the proposed multi-objective VRP4E.

Based on the above, this paper proposes a novel multi-objective ACS algorithm for VRP in epidemics, which is called MOACS4E. In general, by extending the MPMO framework, the MOACS4E uses two independent ant colonies to optimize the travel and prevention costs respectively, so that the two objectives can be searched sufficiently. Besides, the MOACS4E is with two novel and efficient methods, which are a pheromone fusion-based solution generation (PFSG) method and a solution quality improvement (SQI) method. First, as each colony only focuses on its corresponding objective, the central part of the Pareto front may lack enough exploration. Therefore, the PFSG method is proposed to solve this issue. By fusing the pheromone information from different colonies, the PFSG can generate solutions with the consideration of both travel and prevention costs, providing exploration for the central part of the Pareto front. Second, the SQI method is proposed to enhance the solutions for the prevention cost objective, which can improve the optimization efficiency of the MOACS4E.

To sum up, the major contributions of this paper are as follows:

1) This paper proposes a novel multi-objective VRP4E model that takes not only travel cost but also prevention cost into consideration, which can provide significant benefits in combatting the COVID-19 and other similar epidemic outbreaks worldwide. Nevertheless, to the best of our knowledge, this paper is the first that considers the prevention cost of VRP in epidemics. In addition, this paper has also analyzed whether the VRP4E is suitable to be solved via the multi-objective optimization theoretically.

2) An efficient MOACS4E algorithm that integrates ACS and MPMO framework is proposed to solve the proposed multi-objective VRP4E model, where two colonies are utilized to optimize travel and prevention cost objectives, respectively, so as to search the two objectives sufficiently.

3) A novel PFSG method is proposed to better explore the central part of the Pareto front, so that the MOACS4E can produce Pareto solutions with a better tradeoff between the travel and prevention costs.

4) A novel SQI method is proposed to further improve the solution quality for the prevention cost objective, which can improve the efficiency of MOACS4E.

In the experiments, the proposed MOACS4E is investigated on 25 VRP4E problem instances generated based on widely-used VRP benchmarks, where six state-of-the-art algorithms are adopted as contenders. Moreover, visualizations

of the found Pareto front of VRP4E problem instances with different outbreak situations are also provided and analyzed in the paper, which may help provide insightful information for the potential readers from various fields in combatting epidemics. Besides, a real-world case study with data from the Beijing-Tianjin-Hebei region is also conducted for deeper investigation and observations. Therefore, it is expected that this paper can provide great benefits to both the research and application of VRP in epidemics, and more importantly, help save more lives.

The rest contents are provided as follows: Section II gives a brief introduction of the background of the multi-objective problem and VRP, and a review of related work for multi-objective VRPs. Section III formulates the multi-objective VRP for epidemics, while Section IV details the proposed MOACS4E algorithm for solving the multi-objective VRP4E. Section V offers the experiments, including settings, metrics, comparisons, and analyses. In the end, Section VI gives the conclusion.

II. Background and Related Work

A. Multi-Objective Optimization Problem

Generally speaking, a minimization multi-objective problem (MOP) on a search space Ω can be formulated as follows:

$$\text{Minimize} F(x) = [f_1(x), f_2(x), \ldots, f_M(x)] \tag{1}$$

where $x \in \Omega$, F consists of M objective functions f_1, f_2, …, and f_M and maps x from Ω to the objective space Ψ^M, i.e., F: $\Omega \rightarrow \Psi^M$. Given a minimization MOP as Eq.(1), some important concepts about MOP can be defined as follows.

Definition 1 [Pareto Domination]: Given any two vectors $u = [u_1, u_2, \ldots, u_M]$ and $w = [w_1, w_2, \ldots, w_M]$ in the objective space, we say that u **dominates** w if $u_m \leq w_m$ for all $m = 1, 2, \ldots, M$ and $u \neq w$, denoted as $u \prec w$.

Definition 2 [Pareto optimal]: A solution vector $x \in \Omega$ is **Pareto optimal** if there is no $x^* \in \Omega$ such that $F(x^*)$ dominates $F(x)$.

Definition 3 [Pareto set]: The Pareto set (*PS*) is a set of the Pareto optimal solutions, which can be represented as

$$PS = \{x \in \Omega \text{ and } x \text{ is Pareto optimal}\} \tag{2}$$

Definition 4 [Pareto front]: The Pareto front (*PF*) is composed of the solutions in *PS*, as

$$PF = \{F(x) \,|x \in PS\} \tag{3}$$

B. Vehicle Routing Problem

Many VRP variants have been proposed and studied in the past decades [10]. Without loss of generality, this paper employs the CVRP model as the basic model for developing VRP4E. CVRP is one of the most well-known VRP variants in the literature and is similar to VRP except that the vehicle has the capacity [10]. Therefore, compared with the original VRP, the CVRP is not that complex but can be more realistic for real-world applications.

Mathematically, a CVRP can be formulated as follows. Given a connected undirected graph $G=\{V, E\}$ consists of a customer set $V=\{v_i|i = 0, 1, 2, \ldots, N\}$, where N denotes the total number of customers and v_0 is the depot, and an edge set $E = \{e_{ij}|i, j = 0,1, 2, \ldots, N \text{ and } i \neq j\}$. Each edge e_{ij} represents the edge between v_i and v_j. Considering the depot has K available vehicles, a set of demand load for each customer $L=\{load(v_i)|v_i \in V\}$, and a travel cost matrix *trc* where $trc_{i,j}$ represents the travel cost between v_i and v_j, the goal of CVRP is to find a set of vehicle routes $S = \{r_k|k = 1, 2, \ldots, K\}$ with a minimal total travel cost such that:

1) each route r_k must begin and end with the depot v_0 and must be a directed acyclic graph with $|r_k|$–1 edges, where $|r_k|$ is the number of vertexes in r_k;

2) the total load of each r_k can not exceed the available capacity of each vehicle;

3) each v_i $(0 < i \leq N)$ appears only once in S, i.e., each customer should be and only be served once.

Based on the above, the objective function of CVRP for minimizing travel cost can then be defined as:

$$f_{travel}(S) = \sum_{k=1}^{K} tcost(r_k) \tag{4}$$

where $tcost(r_k)$ is the function that summarizes the travel cost of each edge in the route r_k based on the *trc*.

C. Related Work

This part briefly introduces related work on both the aspects of the proposed model and the proposed algorithm.

Firstly, the work related to the proposed model is reviewed. Existing studies about VRP in epidemics can be categorized into two major categories, the approach for epidemic control via VRP and the approach for epidemic control in VRP. The first category mainly focuses on how to control the epidemic via VRP, e.g., urgent transportation and assignment of patients and medical resources [37]–[39]. Therefore, the main challenges concerned in this category are often due to the time constraint, resources and tools shortage, and the demand (which can be dynamic and uncertain) [40]. As this paper is not in this category, the methods in this category are not detailed herein. Different from the first category, the second category considers how to prevent and control epidemics in VRP, so as to perform transportation both safely and efficiently in epidemics. However, not enough attention has been paid to this category yet. The core issue in this category is to reduce the negative influence of the routing plan in epidemics, which will be heavily influenced by the prevention policy during the travel. For example, isolation of the driver and quarantine of the vehicle can be in high demand in such situations because they can help reduce the infection risk. Therefore, to meet the high demand for isolation and quarantine, Majzoubi *et al.* [41] proposed a VRP model where each vehicle can serve up to two patients. Furthermore, Zhang *et al.* [42] studied the efficient high-risk individual transfer with a limited number of quarantine vehicles. Given that the quarantine can prevent the virus spread, Mook *et al.* [43] analyzed the efficiency of quarantine policy for VRP in epidemics. In addition, some studies also cover the issue of social distancing (e.g., the maximum number of customers assigned to each vehicle) [44],

infection risk [45], and possible transmission degree [46]. However, the above VRP models in epidemics consider the VRP from the aspect of how to achieve safety and efficiency, but do not consider the cost in the reality for achieving safety, e.g., the prevention cost. Differently, this paper considers the prevention cost for achieving safety in epidemic situations, which can help bridge the gap between existing research and practice in combatting epidemics. Moreover, note that the proposed model can be regarded as a basic model and then further extended with more issues (e.g., the time-window constraints), so as to become a more suitable or specially-designed model according to the need of users. Therefore, the proposed model is rational and practical, which would have great research and application potential in the community.

Secondly, the work related to the proposed algorithm is reviewed. To date, there have been many works about multi-objective ACS/ACO algorithms for solving traditional transportation problems [27], [47]–[49]. Among them, few multi-population algorithms have obtained promising results in VRP [49]. However, the algorithm proposed in this paper is very different from these existing algorithms in three aspects. First, the existing multi-objective and multi-population ACS/ACO algorithms do not consider how to optimize the prevention cost of the routing plan. For example, the pheromone update in these algorithms does not integrate the information about prevention cost. Therefore, these algorithms are not suitable for solving the VRP with consideration on the prevention cost. Second, to the best of our knowledge, no research has used the MPMO framework to help solve multi-objective VRP (no matter in epidemics or not in epidemics). That is, the proposed algorithm in this paper is the first that attempts to solve the multi-objective VRP problem via MPMO. Third, only few of the existing multi-population ACS/ACO algorithms have adopted pheromone fusion methods [50], [51]. Moreover, all these existing pheromone fusion methods are designed to exchange information among different populations for solving the same objective in the single-objective optimization problem. Differently, the PFSG method is proposed in this paper to exchange the information from populations aiming at different objectives, so as to better explore the central part of the Pareto front. Based on the above, the MOACS4E algorithm proposed in this paper is very novel when compared with existing algorithms and methods.

III. The VRP4E Model

The proposed VRP4E model is a multi-objective CVRP model, where the first objective is the travel cost as represented in Eq.(4) and the second objective is the prevention cost that will be formulated in this part.

During the COVID-19 epidemics, various prevention approaches, such as quarantine and lockdown, have been taken to slow the COVID-19 spreads [17], which can affect the vehicle routing among different regions, cities, and nations seriously. In such cases, the prevention cost should be considered carefully because the prevention cost can differ from route to route greatly. For example, when a driver travels from a high-risk area to a low-risk area, he may be required to spend several hours for COVID-19 testing by the local public health authorities, e.g., viral tests and antibody tests, due to his earlier exposure to COVID-19 in a high-risk area. Even, he may be asked for quarantine to watch for symptoms until 14 days if the local authorities adopt a strict prevention policy. These will result in expensive costs in time and money, e.g., for the testing and the quarantine of the driver in Hotels. Moreover, an additional driver should be employed temporarily to replace the quarantined driver to accomplish the rest transportation tasks so that the goods and products can be delivered on time to the rest customers. For example, to ensure on-time daily deliveries, JD.com's logistics delivered goods and products to Shanghai, China, in 2022 via "suicide logistics" with 14 groups of couriers[52]. That is, the i^{th} batch of couriers needed to be isolated for 14 days after entering high-risk areas of Shanghai on day i, i.e., isolated from day i to day $i+14$, the $(i+1)^{\text{th}}$ batch of couriers continued the transportation the next day and isolated from day $i+1$ to day $i+15$, so as to realize the logistics and transportation on time every day through circulation.

However, this will result in more costs than ordinary cases undoubtfully (e.g., ordinary cases do not need to employ an additional driver). These costs are due to the prevention policy, and therefore can be referred as the prevention cost. Despite the driver, the goods and products in the vehicle may also be unpacked for testing and disinfecting, which will increase cargo damage, especially when the goods are fresh food and frozen goods. Hence, visiting a high-risk area will greatly increase the prevention cost for the following journey. However, if the driver does not visit high-risk areas before, he will just need to take a simpler and quicker temperature measurement and have some visit registrations before entering a new area. That is, the transportation is similar to that in ordinary cases and we do not need the cost of having quarantine and employing an additional driver. In this case, the prevention cost for the following journey is not expensive. That is, visiting high-risk areas will result in high prevention costs for the following journey, while visiting low-risk areas will only have a much cheaper prevention cost for the following journey.

Based on the above, we can formulate the prevention cost of a routing plan as follows. Given a routing solution with K routes, $S=\{r_k|k=1, 2, \ldots, K\}$, the objective function of the prevention cost can be formulated as:

$$f_{prevention}(S)=\sum_{k=1}^{K} pcost(r_k) \tag{5}$$

where the $pcost(r_k)$ is the prevention cost during the k^{th} route (i.e., the route of k^{th} vehicle), and can be formulated as

$$pcost(r_k)=\sum_{i=2}^{|r_k|}(lpc\cdot(1-I(r_k,i))+hpc\cdot I(r_k,i)) \tag{6}$$

where lpc means the low prevention cost if the vehicle has not visited any high-risk area, while hpc denotes the high prevention cost if the vehicle has visited some high-risk areas before. The $I(r_k, i)$ is to indicate whether the vehicle has

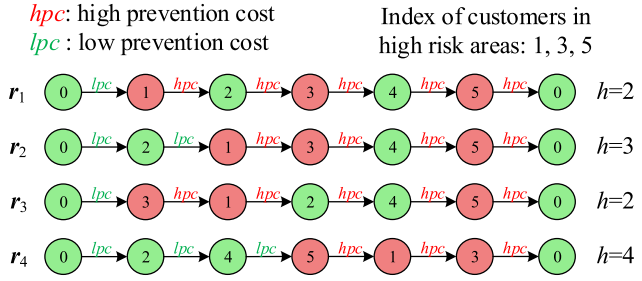

Fig. 2. Example of 4 routes with different prevention costs.

visited any customers in high-risk areas before visiting the i^{th} customer in route r_k, which can be written as

$$I(r_k, i) = \begin{cases} 1, & \text{if } \exists j < i, h(r_k, j) == 1 \\ 0, & \text{otherwise} \end{cases} \tag{7}$$

where $h(r_k, j)$ is to indicate whether the corresponding area of jth vertex in the route r_k is high-risk, and can be written as

$$h(r_k, j) = \begin{cases} 1, & \text{if the } j\text{th vertex in } r_k \text{ is high-risk} \\ 0, & \text{otherwise} \end{cases} \tag{8}$$

where $h(r_k, j) = 1$ indicates that the corresponding area of jth vertex in the route r_k is high-risk, while $h(r_k, j) = 0$ indicates that the corresponding area is low-risk. It should also be noted that the Eq.(6) summarizes the results from $i = 2$ to $i = |r_k|$ because the first vertex in r_k is the depot v_0 and there are only $|r_k|-1$ edge in every r_k. In addition, it is assumed that the depot is in a low-risk area, which is reasonable in that the high-risk epidemic area is often the one that needed to be supported by other areas through transportation systems rather than the one that offers help to other areas.

To make the above contents easier to understand, Fig. 2 gives 4 example routes. As can be seen, during the r_1 in Fig. 2, as the second index is Customer 1 in a high-risk area, i.e., $h(r_1,2)=1$, the prevention costs for visiting the rest customers are all *hpc*. During the r_2, the route first visits Customer 2 in a low-risk area and then visits Customer 1, i.e., the third node is a Customer in a high-risk area (i.e., $h(r_2,3)=1$), therefore both the prevention costs from the depot to Customer 2 and from the Customer 2 to Customer 1 are *lpc* while the rest visiting will have *hpc*. The r_3 is similar to r_1 because the second node is a Customer in high-risk areas. In the r_4, the vehicle will visit all customers in low-risk areas before visiting any customers in high-risk areas. Therefore, this route has $h(r_4, j) = 0$ for $j = 1$, 2, and 3, and only the travel after visiting the fourth area (i.e., Customer 5) will have *hpc*.

To reduce the prevention cost, it is suggested that the vehicle should first visit customers in low-risk areas and then visit the customers in high-risk areas. However, the prevention cost objective can be conflicted with the travel cost objective, because the travel cost objective requires the customers to be visited in an order with the shortest travel distance. Therefore, to minimize such two objectives together, we model this problem as a multi-objective problem, which can be formulated as:

$$\text{Minimize} F_{VRP4E}(S) = [\min f_{travel}(S), \min f_{prevention}(S)] \tag{9}$$

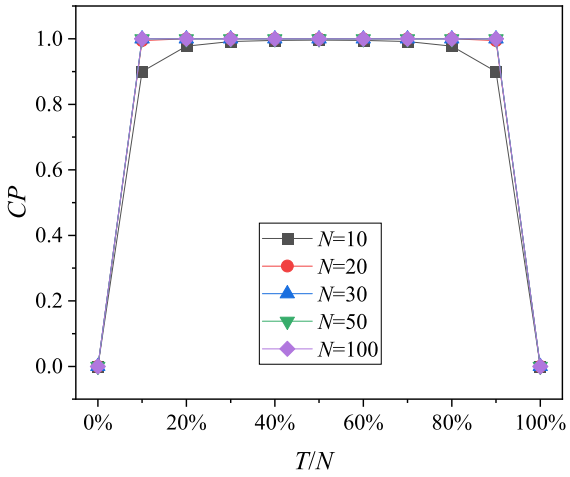

Fig. 3. The confliction probability (CP) with different numbers of total visiting areas and different percentages of high-risk areas.

where the $f_{travel}(S)$ and $f_{prevention}(S)$ are defined as Eq.(4) and Eq.(5), respectively.

Note that the key issue of MOP is that the multiple objectives are conflicted with each other and no solution can get the optima on all objectives at the same time. Therefore, we analyze the confliction probability (*CP*) between the travel cost and the prevention cost herein to show that it is rational and suitable to formulate the VRP4E as a MOP.

Assume that a route visiting N areas (customers) has an optimal travel cost, and T is the number of high-risk areas. Note that the high-risk areas should be visited at the end of the route to get the smallest prevention cost. That is, a route with optimal travel cost can also have optimal prevention cost only if the T high-risk areas are exactly the last T areas visited in the route (only one possible case). Therefore, the probability of the event "the route with optimal travel cost also has the optimal prevention cost" is

$$\frac{1}{\binom{T}{N}} = \frac{1}{\frac{N!}{T!\times(N-T)!}} = \frac{T! \times (N-T)!}{N!} \tag{10}$$

That is, the *CP* of the two objectives can be calculated as:

$$CP = 1 - \frac{1}{\binom{T}{N}} = 1 - \frac{T! \times (N-T)!}{N!} \tag{11}$$

To investigate the *CP*, Fig. 3 plots the *CP* with a different number of visiting areas (i.e., N) and different percentages of high-risk areas (i.e., T/N). As can be seen, unless the high-risk percentage is very close to 0 or 1, the *CP* is very high. That is, the travel and prevention cost objectives have a high probability to be conflicted with each other when there are some high-risk areas. This makes the VRP4E problem complex and difficult to optimize. Therefore, it is suitable to consider the optimization of the two objectives as a MOP.

IV. The Proposed MOACS4E

To solve the VRP4E model described in Section III, this paper proposes the MOACS4E algorithm with the extending

MPMO framework and the PFSG and SQI methods. The following contents will detail the solution encoding, solution construction, pheromone initialization and update, PFSG, SQI, and the complete algorithm one by one.

A. Solution Encoding

To make the solution reproduction more efficient, this paper adopts the efficient solution encoding scheme proposed for single-objective VRP problems in [29]. That is, each solution, representing a candidate S, is encoded as a permutation of all customer indexes and several '0's, where the '0's indicate the depots that partition S into routes r_1, r_2, …, and r_K for K corresponding vehicles. For example, considering a routing for 5 customers, an individual (solution) S ={0, 2, 1, 0, 5, 0, 3, 4, 0} corresponds to a routing plan with 3 routes, i.e., r_1 ={0→2→1→0}, r_2 ={0→5→0}, and r_3 ={0→3→4→0}; while an individual (solution) S ={0, 2, 1, 3, 0, 4, 5, 0} means a solution with 2 routes, i.e., r_1 ={0→2→ 1→ 3→0} and r_2 ={0→ 4→ 5→0}.

Algorithm 1 Solution Construction

Input: τ-the pheromone information of the colony;
N_r- the number of customers;
trc - travel cost between every two customers including depot;
Output: S -the constructed solution.

```
1: Begin
2:   //Step 1
3:     Initialize rest with the indexes of all customers;
4:     Initialize currently-located index j = 0; //begin at depot
5:     Initialize solution S={0};
6:     Initialize L_c =0; //current load
7:     While rest is not empty Do
8:         // Step 2
9:         Compute P_j based on rest according to Eq.(13);
10:        If j==0 Then //if it is the depot
11:          P_j(0)=0; // will not consider the depot
12:        End If
13:        Sample q uniformly within [0,1];
14:        Select next_j according to Eq.(12);
15:        // Step 3
16:        Set j as next_j;
17:        Update current load L_c according to Eq.(14);
18:        Remove next_j from rest;
19:    End While
20: End
```

B. Solution Construction

Imitating the foraging behavior of ants for finding food, ACS constructs solutions efficiently based on pheromone and heuristic information in an iterative fashion. That is, in every solution construction iteration, ACS uses pheromone and heuristic information to determine which customer should be the next one to visit. Moreover, as the total load demand in a route should not exceed the maximum capacity of a vehicle, the load demand is also considered when constructing a solution in MOACS4E.

The pseudo code of solution construction is presented as **Algorithm 1**, which mainly has three steps. Considering N customers, the solution construction through an ant A_i, can be presented as follows.

Step 1: Initialization of the beginning index, i.e., the depot. In this step, A_i is initialized with the route as S_i ={0}, the current load L_c as 0, and an index list of all customers that needed to be visited, denoted as *rest*.

Step 2: Select the next customer to visit. Suppose A_i locates in customer j currently (if it is the depot, j is 0), the algorithm will select one index from the *rest*, based on the probability $P_j(rest\_k)$ for choosing every index $rest\_k \in rest$. Noted that if the currently-located customer j is not the depot, then index set *rest* will include the depot index, otherwise, the *rest* will not consider the depot, so that the cyclic route (e.g., {depot→depot→depot}) can be avoided. To select an index based on P_j, two selection methods, i.e., greedy- and roulette-based methods, are combined with a control parameter q_0. When selecting the index based on P_j, say *next_j*, a random value q is sampled uniformly within [0,1]. If $q \le q_0$, the algorithm will select the index *next_j* with maximum $P_j(next\_j)$; otherwise, the algorithm will select the *next_j* through a roulette wheel selection according to P_j. Mathematically, the selection of *next_j* can be presented as:

$$next\_j = \begin{cases} \arg\max_{rest\_k \in rest} P_j(rest\_k), & \text{if} q \le q_0 \\ roulette(P_j, rest), & \text{otherwise} \end{cases} \quad (12)$$

where *roulette*(P_j, *rest*) will output an index in *rest* based on the roulette wheel selection according to P_j. Noted that if $q \le q_0$(i.e., in greedy-based selection) and some customers have the same P_j value, the first one in the list will be selected.

The $P_j(rest\_k)$ is calculated based on pheromone $\tau_{j,rest\_k}$, and the heuristic information $\eta_{j,rest\_k}$ and $\theta_{j,rest\_k}$, which can be written as:

$$P_j(rest\_k) = \begin{cases} \frac{\tau^{\alpha}_{j,rest\_k} \times \eta^{\beta}_{j,rest\_k} \times \theta^{\gamma}_{j,rest\_k}}{\sum_{z \in rest} \tau^{\alpha}_{j,z} \times \eta^{\beta}_{j,z} \times \theta^{\gamma}_{j,z}}, & \text{if } load\ (rest\_k) \\ & +L_c \le Capacity \\ 0, & \text{otherwise} \end{cases} \quad (13)$$

where a larger $\eta_{j,rest\_k} = 1/trc_{j,rest\_k}$ means a smaller travel cost between customer j and *rest_k*, a larger $\theta_{j,rest\_k} = trc_{j,0} + trc_{0,rest\_k} - trc_{j,rest\_k}$ indicates visiting *rest_k* after j in a route can be more desired than separating them into different routes. Besides, the α, β, and γ are parameters for controlling the influence of pheromone and heuristic information on selecting the next customer to be visited. It should also be noted that the Eq.(13) can still work well when the vehicle is nearly fully-loaded and cannot serve any more customers, because in this situation, Eq.(13) will set P_j of all the rest customers as 0 except the depot. In such a situation, the depot will be surely selected because only the depot has a positive probability, i.e., $P_j(0) > 0$, which means that the construction of the current route will be finished and the next route is to begin.

Step 3: Complete the solution. After choosing the *next_j*, the algorithm will update the corresponding construction information by setting the currently-located index j to be *next_j*,

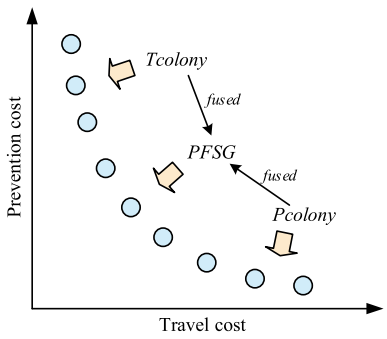

Fig. 4. The roles of Tcolony, Pcolony, and PFSG in the proposed algorithm for finding the Pareto front.

removing *next_j* from *rest*, and updating the current load as

$$L_c = \begin{cases} L_c + load(next\_j), & \text{if } next\_j \text{ is not the depot} \\ 0, & \text{otherwise} \end{cases} \quad (14)$$

Then, if there are still some customers in *rest*, the algorithm will go back to Step 2 and continue selecting the next customer. Otherwise, the solution construction finishes.

C. Pheromone Initialization and Update

In the proposed algorithm, two ant colonies use different pheromones for minimizing different objectives correspondingly. For simplicity, this paper denotes the colonies for the travel and prevention cost objectives as *Tcolony* and *Pcolony*, respectively. Following this, $\tau^{Tcolony}$ and $\tau^{Pcolony}$ are used to denote the pheromones in colonies *Tcolony* and *Pcolony*, respectively. Noted that when constructing a solution in the *Tcolony* or the *Pcolony* population, the τ in Eq. (13) is replaced by $\tau^{Tcolony}$ or $\tau^{Pcolony}$, respectively. The pheromone initialization and update process are described as follows.

1) Pheromone Initialization

In the proposed algorithm, the initial pheromone values for *Tcolony* and *Pcolony* are defined as Eq.(15) and Eq.(16), respectively.

$$\tau_0^{Tcolony} = \frac{1}{f_{travel}(S_{TG})} \quad (15)$$

$$\tau_0^{Pcolony} = \frac{1}{f_{prevention}(S_{PG})} \quad (16)$$

where S_{TG} and S_{PG} are the greedy solutions for *Tcolony* and *Pcolony*, respectively. The construction process of S_{TG} is the same as that described in previous Section IV-B, except that only the greedy-based method is used to select the next customer to be visited, i.e., $q_0 = 1$ in Eq. (12), and therefore the customer with the largest P_j will be selected as the next one every time. Moreover, the generated solution will then be further enhanced by the classical and widely-used 2-*opt* local search method [53], [54], which results in the final S_{TG}. The S_{PG} is improved from S_{TG} by using SQI, where the SQI will be described in Section IV-E.

2) Pheromone Local Update

When an ant completes the construction of a solution, the solution will be used to perform the pheromone local update immediately. It should be noted that the solution construction process of *Tcolony* and *Pcolony* are independent of each other, which provides an advantage that they can use different pheromone values (including initial value and updated value) to minimize their objective correspondingly.

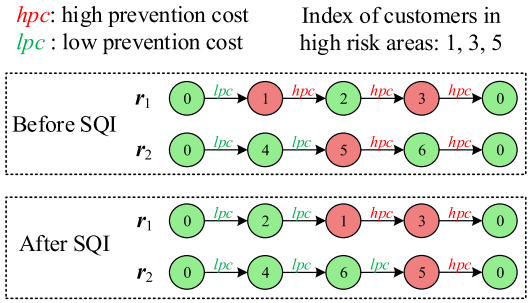

Fig. 5. Example of two routes before and after the SQI.

The local update process of pheromone for *Tcolony* and *Pcolony* are in the same way, which updates the pheromone value on the visited edge. For example, if *next_j* is the next customer to be visited after visiting j in the solution S_i which is newly generated in *Tcolony* (or *Pcolony*), then the related pheromones in *Tcolony* (or *Pcolony*) are updated as Eq.(17) (or Eq.(18)), respectively.

$$\tau_{j,next\_j}^{Tcolony} = (1-\rho) \times \tau_{j,next\_j}^{Tcolony} + \rho \times \tau_0^{Tcolony} \quad (17)$$

$$\tau_{j,next\_j}^{Pcolony} = (1-\rho) \times \tau_{j,next\_j}^{Pcolony} + \rho \times \tau_0^{Pcolony} \quad (18)$$

where $\rho \in [0,1]$ is a parameter to control the change rate of the pheromone value.

3) Pheromone Global Update

The pheromone global update for *Tcolony* and *Pcolony* is based on the current best solutions for the travel and prevention objectives respectively (i.e., S_T and S_P), as represented as:

$$\tau_{j,next\_j}^{Tcolony} = (1-\rho) \times \tau_{j,next\_j}^{Tcolony} + \rho \times \frac{1}{f_{travel}(S_T)} \quad (19)$$

$$\tau_{j,next\_j}^{Pcolony} = (1-\rho) \times \tau_{j,next\_j}^{Pcolony} + \rho \times \frac{1}{f_{prevention}(S_P)} \quad (20)$$

Algorithm 2 Solution Quality Improvement

Input: S-the solution to be improved;
Output: S_{impr} -the improved solution.
Begin
  Split S into several routes according to the number of "0" in S;
  Store the obtained routes in *Routes*;
  For each route r_i in *Routes***Do**
    Initialize *mid* as an empty set;
    For each index j in r_i**Do**
      If $h(r_i, j) == 1$ **Then //**the definition of $h(r_i, j)$ refer to Eq.(8)
        Add j into *mid*;
      End If
    End For
    Move indexes of r_i that are in *mid* to the end of r_i;
  End For
  Merge all the routes in *Routes* to form S_{impr};
End

D. Pheromone Fusion-Based Solution Generation

The PFSG is proposed to fuse the pheromone information from *Tcolony* and *Pcolony* to generate solutions with both

small travel and prevention costs, so as to explore the central part of the Pareto front. For a better illustration, Fig. 4 shows the roles of *Tcolony*, *Pcolony*, and PFSG in the proposed algorithm for finding the Pareto front.

The solution construction in PFSG is the same as that described in previous Section IV-B, except that the adopted pheromone in Eq. (13) is fused by the pheromones in *Tcolony* and *Pcolony*. The fused pheromone, say τ^{fused}, can be obtained as:

$$\tau^{fused} = \lambda \times \sigma^{Tcolony} + (1-\lambda) \times \sigma^{Pcolony} \tag{21}$$

where $\sigma^{Tconlny}$ and $\sigma^{Pconlny}$ are the normalized versions of $\tau^{Tconlny}$ and $\tau^{Pconlny}$, respectively, and their normalization processes are in the same way and can be represented as

$$\sigma_{i,j} = \frac{\tau_{i,j}}{\sum_{z=0}^{N} \tau_{i,z}} \tag{22}$$

where 0 is the depot index. Furthermore, the λ in Eq.(21) is a uniformly distributed random value within [0,1] for generating different τ^{fused}, so that different solutions can be generated based on different τ^{fused}. This can increase the diversity of generated solutions for exploring the central part of the real Pareto front more evenly.

E. Solution Quality Improvement

The SQI is proposed to improve the solution for the prevention cost. If the solution is generated in *Pcolony*, the algorithm will further improve this solution before evaluating its objective value. To be specific, for each route in the solution, the customers in high-risk areas will be moved to the end of the route in order. For better illustration, Fig. 5 gives the example of two routes before and after the SQI. Considering that when customers 1, 3, and 5 are in high-risk areas, for a solution with two routes $r_1 = \{0 \rightarrow 1 \rightarrow 2 \rightarrow 3 \rightarrow 0\}$ and $r_2 = \{0 \rightarrow 4 \rightarrow 5 \rightarrow 6 \rightarrow 0\}$, the improved solution after SQI can be with two new routes $r_1 = \{0 \rightarrow 2 \rightarrow 1 \rightarrow 3 \rightarrow 0\}$ and $r_2 = \{0 \rightarrow 4 \rightarrow 6 \rightarrow 5 \rightarrow 0\}$. As can be seen in Fig. 5, the routes after SQI can have less *hpc*, which will result in a lower total prevention cost. The pseudo code of SQI is presented as **Algorithm 2**. In **Algorithm 2**, lines 2 and 3 split the solution into several routes, and lines 4 to 12 move the high-risk customers to the end of the corresponding route. Finally, the improved routes are merged to form the improved complete solution S_{impr}, as shown in line 13 of **Algorithm 2**.

F. The Complete Algorithm

Fig. 6 presents the flowchart of the complete MOACS4E, and the corresponding pseudo code is given in **Algorithm 3**. After the initialization, the evolution process of MOACS4E mainly includes the solution generation in *Tcolony*, *Pcolony*, and PFSG, as can be seen in lines 7 to 32 in **Algorithm 3**. All the generated solutions will be measured by two objective functions and then used to update their corresponding pheromones. Note that if a solution violates the constraints (e.g., exceeding the maximum number of available vehicles), both the two objective values will be set as a large value (e.g., 1×10^{25}). To obtain the Pareto set, all the generated solutions will be stored in an *Archive*. At the end of each generation, the *Archive* will drop solutions that are denominated by other solutions in the *Archive*, as shown in line 27 of **Algorithm 3**. The evolution process will repeat until the stop criteria are met. Finally, the *Archive* that contains the non-dominated solutions will be output, and then the algorithm finishes.

Algorithm 3 The Complete MOACS4E

1: **Begin**
2: Generate and evaluate greedy solution S_{TG} and S_{PG};
3: Store S_{TG} and S_{PG} into an empty set *Archive*;
4: Initialize $\tau^{Tcolony}$ and $\tau^{Pcolony}$ according to Eq.(15) and Eq.(16);
5: Initialize $S_T = S_{TG}$; //the best solution for travel objective
6: Initialize $S_P = S_{PG}$; //the best solution for prevention objective
7: **While** stop criteria are not met**Do**
8: **For** each ant A_i in *Tcolony***Do**
9: Generate solution S_i based on $\tau^{Tcolony}$; **//Algorithm 1**
10: Evaluate S_i and store it in *Archive*;
11: /* Pheromone local update in *Tcolony*/
12: Update $\tau^{Tcolony}$ according to Eq.(17);
13: **End For**
14: **For** each ant A_i in *Pcolony***Do**
15: Generate solution S_i based on $\tau^{Pcolony}$; **//Algorithm 1**
16: Improve $S_i$for prevention objective; **//Algorithm 2**
17: Evaluate S_i and store it in *Archive*;
18: /* Pheromone local update in *Pcolony*/
19: Update $\tau^{Pcolony}$ according to Eq.(18);
20: **End For**
21: /* PFSG */
22: Normalize $\tau^{Tcolony}$ to be $\sigma^{Tconlny}$;
23: Normalize $\tau^{Pcolony}$ to be $\sigma^{Pcolony}$;
24: Sample λ in [0,1] and compute τ^{fused} according to Eq.(21);
25: Generate solution S_{fused} based on τ^{fused}; **//Algorithm 1**
26: Evaluate S_{fused} and store it in *Archive*;
27: Drop dominated solutions in *Archive*;
28: /* Pheromone global update */
29: Update $S_T$and $S_P$based on *Archive*; //update best solutions
30: Update $\tau^{Tcolony}$ with S_T according to Eq.(19);
31: Update $\tau^{Pcolony}$ with S_P according to Eq.(20);
32: **End While**
33: **End**

Output: All non-dominated solutions in *Archive*.

V. Experimental Studies

A. Problem Instances

To obtain problem instances for the proposed VRP4E model, this paper extends widely-used CVRP instances by selecting some customers to be high-risk randomly. In particular, the number of randomly-selected high-risk customers is configured as the maximum integer smaller than $N \times 10\%$. Table I provides the details of the 25 generated VRP4E instances used in this paper, including the customer number (denoted as N), vehicle number, the capacity of vehicles, and the number of high-risk customers. As can be seen, the 25 instances are with different characteristics such as N and therefore they can help observe how the proposed algorithm will perform in various scenarios. In the experiments, the *hpc* and *lpc* are set as 10 and 1, respectively, so as to emphasize the significant influence of visiting high-risk areas. Besides, all the original CVRP instances can be downloaded online (http://akira.ruc.dk/~keld/research/LKH-3/).

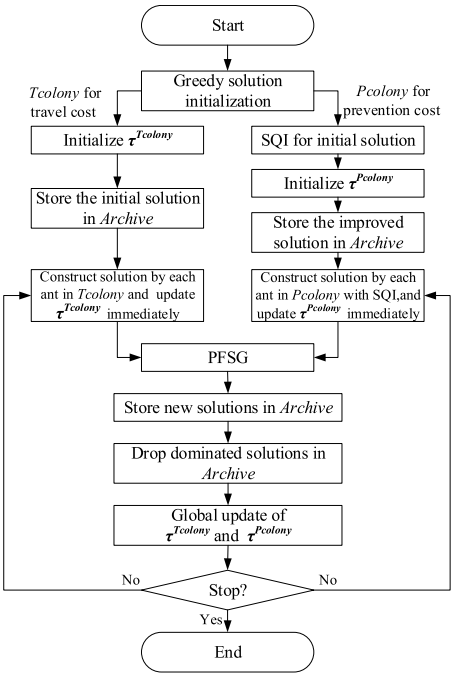

Fig. 6. Flowchart of the complete MOACS4E.

TABLE I
THE PROPERTIES OF 25 TEST PROBLEMS INSTANCES

Problem ID	Basic CVRP instance	Customer Number	Vehicle Number	Vehicle Capacity	Number of High-risk Customers
P01	A-n55-k9	55	9	100	5
P02	A-n60-k9	60	9	100	6
P03	A-n65-k9	65	9	100	6
P04	A-n69-k9	69	9	100	6
P05	A-n80-k10	80	10	100	8
P06	B-n50-k8	50	8	100	5
P07	B-n57-k7	57	7	100	5
P08	B-n63-k10	63	10	100	6
P09	B-n67-k10	67	10	100	6
P10	B-n78-k10	78	10	100	7
P11	E-n51-k5	51	5	160	5
P12	E-n76-k7	76	7	220	7
P13	E-n76-k15	76	15	100	7
P14	E-n101-k8	101	8	200	10
P15	E-n101-k14	101	14	112	10
P16	F-n45-k4	45	4	2010	4
P17	F-n72-k4	72	4	30000	7
P18	F-n135-k7	135	7	2210	13
P19	P-n51-k10	51	10	80	5
P20	P-n55-k15	55	15	70	5
P21	P-n60-k15	60	15	80	6
P22	P-n65-k10	65	10	130	6
P23	P-n70-k10	70	10	135	7
P24	P-n76-k5	76	5	280	7
P25	P-n101-k4	101	4	400	10

B. Performance Metrics

As the real Pareto fronts of the test instances are unknown, some performance metrics based on Pareto fronts, e.g., the inverted generational distance, can not be calculated. Therefore, this paper adopts two widely-used performance metrics that do not require Pareto front data for evaluating and comparing algorithms. The two adopted metrics are hypervolume and set coverage, i.e., HV and C [55]. HV calculates the volume between the solution set and a reference point. The reference point is constructed with the worst values about the two objectives among all solutions produced by all algorithms in all runs. Therefore, the larger the HV value an algorithm has, the better performance an algorithm has. Differently, C measures the degree of how much a solution set dominates another set. Given two solution sets U and W, the $C(U, W)$ can be calculated as

$$C(U,W) = \frac{|\{w \in W \,|\exists u \in U \,:\, u\text{dominates}w\}|}{|W|} \tag{23}$$

where $|W|$ means the number of solutions in set W.

C. Compared Algorithms and Experimental Settings

As the VRP4E model is firstly proposed in this paper and no other algorithms have been designed for it, we can only adapt some widely-used and state-of-the-art multi-objective algorithms and apply them to solve the VRP4E model for comparisons. To be specific, this paper adopts six algorithms, which are NSGA-II [56], MOEA/D [57], TS-MOEA [58], coevolutionary constrained multi-objective optimization (CCMO) [59], multi-objective local search (MOLS)[60], ant colony algorithm (ACA) [48] and multi-objective ACO (MOACO) [49]. The NSGA-II and MOEA/D are well-known and widely-used state-of-the-art approaches for multi-objective optimization and have been also widely researched in various multi-objective VRP variants [10], while the TS-MOEA is a currently-proposed two-stage multi-objective algorithm that combines the NSGA-II and MOEA/D for multi-objective VRP problems. Moreover, the CCMO and MOLS are also recently-proposed efficient algorithms for multi-objective VRP. Besides, the ACA and MOACO are also recent multi-objective ACO/ACS algorithms for multi-objective VRPs. Therefore, these algorithms with various characteristics are ideal to compare the proposed algorithm.

For the algorithm settings, MOACS4E sets the commonly-seen parameters for pheromone as $\alpha = 1$, $\beta = 3$, $\gamma = 2$, and $\rho = 0.15$, as suggested in the literature about using ACS for solving VRP problems [29]. Furthermore, the population size of both *Tcolony* and *Pcolony* is set as 50, i.e., the total population size is 100. For fair comparisons, the population size of peer algorithms is also set as 100. In addition, the rest hyperparameters of peer algorithms are set according to their original papers.

In the experiments, all algorithms will be executed with 30 independent runs on each problem and the average results will be used for companions, so that the statistical error can be reduced. For the sake of fairness, the maximum number of fitness evaluations is set as 1×10^5 for each algorithm in each run. In addition, this paper uses the Wilcoxon's rank sum test with a significant level $\alpha = 0.05$ to compare the algorithm results [27]. Based on the Wilcoxon's rank sum test, the symbols '+', '≈', and '-' are used to denote that the proposed algorithm can perform significantly better than, similar to, and significantly worse than other algorithms.

D. Experimental Comparisons

In this part, the proposed MOACS4E is firstly compared with non-metaheuristic methods and then multi-objective opti-

TABLE II
COMPARISONS WITH THE GREEDY METHODS

Problem ID	Average travel cost of each route		Average prevention cost of each route	
	MOACS4E	GreedyT	MOACS4E	GreedyP
P01	**134.198**	153.171	**13.919**	14.889
P02	**173.750**	215.882	**15.441**	17.444
P03	**148.336**	195.434	**16.026**	19.111
P04	**146.576**	190.498	**16.444**	18.444
P05	**206.877**	230.893	**18.460**	20.500
P06	**169.872**	188.273	**14.875**	17.125
P07	**197.333**	274.252	**17.267**	19.286
P08	**171.173**	206.554	**14.203**	17.000
P09	**121.733**	156.121	**14.510**	16.500
P10	**142.243**	194.715	**17.600**	18.500
P11	**118.063**	131.400	**22.340**	25.400
P12	**112.293**	132.043	**22.157**	27.000
P13	**77.679**	94.289	**11.780**	12.467
P14	**119.985**	143.295	**26.875**	30.250
P15	**90.541**	116.162	**16.960**	19.571
P16	**239.352**	262.854	**22.625**	23.250
P17	**68.061**	88.495	**38.067**	39.000
P18	**200.791**	245.853	**40.571**	43.143
P19	**83.047**	114.566	**11.300**	14.000
P20	**68.746**	77.626	**8.684**	9.267
P21	**71.599**	79.783	**9.560**	12.000
P22	**89.345**	108.696	**14.920**	16.300
P23	**95.678**	107.010	**15.900**	20.500
P24	**142.032**	176.051	**31.240**	34.000
P25	**198.203**	225.002	**53.000**	55.250

mization methods, where the results are given and analyzed as follows.

1) *Comparison with Non-Metaheuristic Methods*: Greedy heuristic method is an efficient non-metaheuristic algorithm for solving single-objective problems. Therefore, the greedy method is adopted to compare the proposed MOACS4E. For simplicity, the greedy methods for the travel objective and the prevention objective are denoted as GreedyT and GreedyP, respectively. Noted that the processes of GreedyT are the same as that described in Section IV-C for generating the initial solutions for *Tcolony*, while the solution of GreedyP is initialized randomly and then is improved by SQI to minimize its prevention objective value. Note that MOACS4E is a multi-objective algorithm whose output is a solution set containing multiple solutions in a run. Therefore, for each objective, the solution with the best value on this corresponding objective is regarded as the best solution found by MOACS4E, and the mean result of the best solutions on this objective in all the runs is compared with the solution obtained by the greedy method.

Table II presents the comparison results between MOACS4E and two greedy methods, where the better results are marked in **boldface**. As can be seen in Table II, the proposed MOACS4E can obtain smaller travel and prevention costs than greedy methods on all problem instances. This suggests that MOACS4E is effective for producing more satisfactory solutions. Moreover, the Fig. S.1 of the supplementary material provides the convergence curve of the proposed MOACS4E algorithm on the travel cost objective and the prevention cost objective of P01. As can be seen from Fig. S.1, the MOACS4E can quickly converge on the two objectives, which further shows the optimization efficiency of the MOACS4E.

2) *Comparison with Multi-Objective Methods*: The comparison results of *HV* and *C* metrics between MOACS4E and state-of-the-art multi-objective algorithms are given in Table III and Table IV, respectively. The detailed comparison results of Table III and Table IV and given in Table S.I and Table S.II of the supplementary material, respectively. As shown in Table III, according to the Wilcoxon's rank sum test, the proposed MOACS4E can obtain significantly better HV values on at least 18 problems than all compared algorithms. Moreover, Table IV shows that most solutions obtained by the MOACS4E can dominate the solutions produced by the compared algorithms on most problem instances, which suggest that the MOACS4E can outperform the compared algorithms in term of the set coverage metric. It is no surprise that the proposed MOACS4E can outperform the compared algorithms, because the MOACS4E is proposed for solving the proposed VRP4E problem while the compared algorithms are originally designed for other multi-objective VRP variants. In conclusion, the comparison results have verified the effectiveness of the proposed MOACS4E.

E. Component Analysis

This part analyzes the components of MOACS4E experimentally, including the *Tcolony* for travel cost objective, the *Pcolony* for prevention cost objective, the PFSG for producing more solutions on the Pareto fronts, and SQI for solution improvement. Therefore, this part compares MOACS4E and its variants without *Tcolony*, without *Pcolony*, without PFSG, and without SQI. For the sake of simplicity, the four variants are denoted as 'MOACS4E-w/o-T', 'MOACS4E-w/o-P', 'MOACS4E-w/o-PFSG', and 'MOACS4E-w/o-SQI', respectively. In the implementation, the MOACS4E-w/o-T only evolves a population for optimizing prevention cost, while the MOACS4E-w/o-P only evolves a population for optimizing traversal cost. Moreover, the PFSG, which is based on two populations for different objectives, is not included in either 'MOACS4E-w/o-T' or 'MOACS4E-w/o-P'. Other parameter settings of 'MOACS4E-w/o-T' and 'MOACS4E-w/o-P' are the same as MOACS4E.

The comparisons between the MOACS4E and its variants are given in Table V, where the detailed companion results can be seen in Table S.III of the supplementary material. As shown in Table V, according to the Wilcoxon's rank sum test with a significant level $\alpha = 0.05$, the MOACS4E significantly outperforms MOACS4E-w/o-T, MOACS4E-w/o-P, MOACS4E-w/o-PFSG, and MOACS4E-w/o-SQI on 18, 25, 17, and 25 problems, respectively, and performs significantly worse on none problems. Moreover, Table S.III shows that the MOACS4E obtains the best results (as marked in **boldface**) among the variants on all problem instances. These suggest that each component has its contribution to the great effectiveness of MOACS4E and dropping any of them will degrade the algorithm performance. Besides, it can be seen that the MOACS4E outperforms MOACS4E-w/o-PFSG on fewer problems than those of other variants. This indicates that the travel cost objective and prevention cost objective can be conflicted with each other heavily, and therefore only a

TABLE III

COMPARISON RESULTS BETWEEN MOACS4E AND STATE-OF-THE-ART ALGORITHMS BASED ON HYPERVOLUME

Statistical Item	NSGA-II	MOEA/D	TS-MOEA	CCMO	MOLS	ACA	MOACO
MOACS4E is significantly better on	**21**	**25**	**25**	**19**	**19**	**18**	**18**
Two algorithms are similar on	1	0	0	2	2	2	2
MOACS4E is significantly worse on	3	0	0	4	4	5	5

TABLE IV

COMPARISON RESULTS BETWEEN MOACS4E AND STATE-OF-THE-ART ALGORITHMS BASED ON SET COVERAGE

Statistical Item.	A1=MOACS4E vs A2=NSGA-II		A1=MOACS4E vs A2=MOEA/D		A1=MOACS4E vs A2=TS-MOEA		A1=MOACS4E vs A2= CCMO		A1=MOACS4E vs A2= MOLS		A1=MOACS4E vs A2= ACA		A1=MOACS4E vs A2= MOACO	
	C(A1, A2)	*C*(A2, A1)	*C*(A1, A2)	*C*(A2, A1)	*C*(A1, A2)	*C*(A2, A1)	*C*(A1, A2)	*C*(A2, A1)	*C*(A1, A2)	*C*(A2, A1)	*C*(A1, A2)	*C*(A2, A1)	*C*(A1, A2)	*C*(A2, A1)
# best	**19**	6	**25**	0	**24**	1	**17**	8	**17**	8	**18**	7	**17**	8

Symbols "A1" and "A2" are used to represent the corresponding algorithms for brevity.

TABLE V

COMPARISONS BETWEEN MOACS4E VARIANTS BASED ON HYPERVOLUME FOR COMPONENT ANALYSIS

Statistical Item	MOACS4E-w/o-T	MOACS4E-w/o-P	MOACS4E-w/o-PFSG	MOACS4E-w/o-SQI
Original MOACS4E is significantly better	**18**	**25**	**17**	**25**
Two algorithms are similar	7	0	8	0
Original MOACS4E is significantly worse	0	0	0	0

TABLE VI

COMPARISONS BETWEEN MOACS4E VARIANTS WITH DIFFERENT PARAMETERS IN PFSG BASED ON HYPERVOLUME

Statistical Item	Original λ	λ=0.3	λ=0.5	λ=0.7
Original λ is significantly better	NA	0	0	0
Two algorithms are similar	NA	25	25	25
Original λ is significantly worse	NA	0	0	0
Number of best results	**10**	6	6	8

few non-dominated solutions with both low travel and prevention costs can be found even though the PFSG is adopted. In addition, the MOACS4E-w/o-P and MOACS4E-w/o-SQI perform worse than other MOACS4E variants, which suggests that the *Pcolony* and SQI have more contribution than other components. Overall, the experimental results have verified the benefits of the components in the proposed MOACS4E.

F. Parameter Study

Compared with existing ACS variants for VRP problems, the additional parameter in MOACS4E is the λ in PFSG. As can be seen in Eq.(21), the λ controls the preferences of pheromones in *Tcolony* and *Pcolony* for producing high-quality solutions. Therefore, this part compares MOACS4E with its variants using different λ. As the original λ is uniformly generated within [0, 1] at every generation, the compared variants use fixed $\lambda = 0.3$, $\lambda = 0.5$, and $\lambda = 0.7$. The comparison results of HV are given in Table VI, whereas the detailed results are provided in Table S.IV of the supplementary material. As can be seen in Table VI, the original λ has similar results with different λ values based on the Wilcoxon's rank sum test, which suggests the performance of MOACS4E is not sensitive to the parameter λ. This may be because that the Pareto front is not continuous and therefore different parameters do not have significant differences in producing the solutions for the central part of the Pareto front. However, the results also show that the original λ can obtain the best results on 10 problems, while the variants with λ =0.3, $\lambda = 0.5$, and $\lambda = 0.7$ only gained the best results on 8, 6, 8 problems, respectively, which verify the effectiveness of the original configuration. Based on the above, the performance of the proposed algorithm is not sensitive to the parameter λ and the original setting of λ is recommended.

G. Model Analysis of VRP4E in Different Situations

To provide further analysis of the VRP4E, this part visualizes the Pareto front of VRP4E in different epidemic situations, i.e., with different percentages of high-risk customers. Noted that Pareto fonts of the VRP4E instances are unknown and we can only use the solutions produced by algorithms to approximate the Pareto front. Therefore, the solutions produced by all the algorithms are collected to approximate the Pareto fronts for visualization. Noted that only the non-dominated solutions in the collected set will be plotted, where the set contains the solutions produced by all algorithms in all runs.

Fig. 7 plots the found Pareto solutions on P01 to P04 with different percentages of high-risk customers. From Fig. 7, we can obtain two important observations. First, the found Pareto fronts are not continuous with a considerable gap in the central part of the Pareto front. This may be because that the travel and prevention cost objective are conflicted with each other and it is hard to find solutions that have both small travel and prevention costs. Therefore, it is suitable and recommended to consider these two conflict objectives in a multi-objective problem, so as to obtain a set of high-quality and non-dominated candidate solutions for applications. Second, when choosing the solution with consideration of both travel and prevention costs, the scenarios that some customers are in high-risk areas (e.g., 30% or 50% are high risks) can be more challenging than the scenarios that most customers are

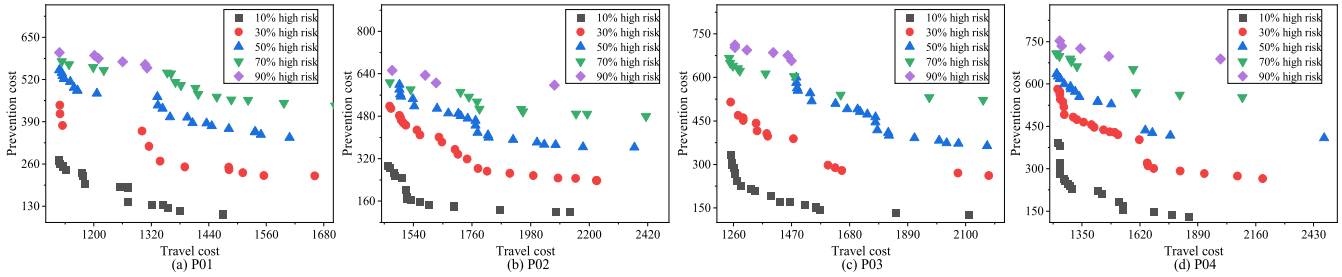

Fig. 7. The found Pareto solutions on VRP4E with different percentages of high-risk customers (a) P01; (b) P02; (c) P03; and (d) P04.

TABLE VII
COMPARISONS OF MEAN RESULTS ON THE REAL-WORLD CASE INSTANCE

Category	Algorithm	HV value	Average travel cost per route (km)	Average prevention cost per route (driver days)
Multi-objective optimization methods	MOACS4E	**5.81E-01**	**629.65**	**12.25**
	NSGA-II	4.09E-01	679.37	18.75
	MOEA/D	1.41E-01	1708.96	16.34
	TS-MOEA	3.26E-01	1388.59	18.09
	CCMO	5.52E-01	646.08	12.90
	MOLS	5.48E-01	646.09	13.55
	ACA	5.57E-01	647.09	16.55
	MOACO	5.46E-01	653.39	13.63
Single-objective optimization methods	SACO	3.85E-01	650.79	19.50
	GreedyT	1.21E-01	1590.18	32.40
	GreedyP	1.25E-01	2529.56	19.05

Note that the average travel cost and the average prevention cost are the best total travel cost and the best total prevention cost divide the number of routes, i.e., number of vehicles, respectively. 1 driver day equals to 1 workday of 1 driver.

in high-risk areas (e.g., 90% are high risks), which is consistent with the analysis in Section III. As shown in Fig. 7, the range of the prevention cost of non-dominated solutions in 30% high-risk scenarios is larger than those in 70% or 90% high-risk scenarios. That is, if the percentage of high-risk are not closer to 0 or 1, the two objectives are conflicted with each other heavily. Based on the above, if the epidemic outbreaks and clusters occur in some areas rather than almost all areas (i.e., the percentage of high-risk areas is between 0 to 1), which are possibly the common cases in the post-COVID-19 period, emphasis should be paid to the prevention cost of routing plans. In such scenarios, it is recommended to consider the travel and prevention costs as two objectives in a multi-objective problem model to obtain higher-quality solutions.

H. A Case Study on Real-World VRP4E

This part conducts a case study on a VRP4E problem with real-world data. As there were local COVID-19 epidemics reported in the Beijing-Tianjin-Hebei region, China, at the beginning of 2021, we consider the VRP4E with the data of this region for the case study. Noted that herein the Beijing-Tianjin-Hebei (pronounced as 'Jing-Jin-Ji' in Chinese) region refers to the whole province-level region of Beijing, Tianjin, and Hebei in China. According to the COVID-19 Prevention and Control Plan (7th Edition) issued by the State Council of China [61], all local authorities of the county-level regions (based on the regional division standard) are required to adjust their epidemic risk level dynamically and make it known on time. As the Beijing-Tianjin-Hebei region consists of 199 county-level administrative regions, including 16 in Beijing, 16 in Tianjin, and 167 in Hebei, these 199 county-level regions are considered as the customers needed to be served. Moreover, according to the corresponding health commission of Beijing, Tianjin, and Hebei, people who have visited high-risk or medium-risk county-level regions may be placed under concentrated quarantine for 7 to 14 days for health observation based on the actual situations, while people from low-risk regions can travel normally with the "green code" of health passcode and a negative nucleic acid test if their temperature detection is normal. That is, the time cost is the main prevention cost in this VRP4E case, and the prevention cost after visiting high-risk or medium-risk county-level regions is similar. Hence, we set the prevention cost after visiting both high-risk and medium-risk county-level regions as hpc=7 while the prevention cost after visiting low-risk county-level regions as lpc=0.5 (about half a day to get the nucleic acid test result). The unit of hpc and lpc is driver day, where one driver day means one workday of one driver. Note that the medium-risk and high-risk county-level regions conduct the same prevention approach, the medium-risk regions are also regarded as high-risk herein. As for the travel cost objective, we directly consider the total travel distance of the candidate routes. Without loss of generality, we set the location of Beijing (i.e., the capital city of China) as the depot. Also, Beijing is low-risk at that time. All the location and travel distance data about the 199 county-level regions and the depot can be obtained from the API provided by Amap [62], where the data distribution can be seen in Fig. 8. Moreover, Fig. 8 also marks the locations of low-risk regions, high-risk regions, and the depot (i.e., Beijing) with red, green, and black color, respectively, where 182 and 17 county-level regions are high-risk and low-risk, respectively, according to the report of local authorities in Beijing-Tianjin-Hebei region on January 19, 2021. As for the demand and car capacity, we set that every county-level region requires 10 units of material and the car capacity is 100 units, because the regions of the same level often have similar demands during the epidemics. The maximum number of vehicles is set as 20.

In the experiment, the multi-objective and greedy methods used in the previous contents are adopted for comparison. Besides, to provide a deeper analysis of the real-world VRP4E, we also add an efficient single-objective ACO (SACO) variant [29] in the comparison, which only uses the travel cost objective. The comparison results are shown in Table VII. From Table VII, three observations can be obtained. First,

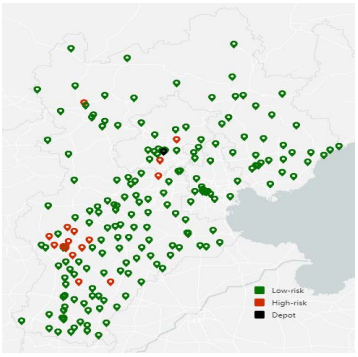

Fig. 8. Visualization of the real-world data for all the 199 divisions in the Beijing-Tianjin-Hebei region.

MOACS4E obtains the best HV value, travel cost, and prevention cost among all the compared algorithms, showing its superior performance. Second, multi-objective methods such as MOACS4E and NSGA-II can outperform the compared single-objective methods, which again supports that multi-objective methods are more suitable for solving the VRP4E. Third, as the MOACS4E significantly outperforms other algorithms including the greedy algorithm, the solutions obtained by MOACS4E can be more practical than the compared algorithm in the real world. Concluding from the above, the effectiveness of MOACS4E in solving the VRP4E is verified in the real-world case study.

In addition, the visualization of the two solutions is shown in Fig. S.2 of the supplemental material. As can be seen in Fig. S.2, the solution with the best travel cost has more separate routes than the solution with the best prevention cost on the top area of the map. This is because that the high-risk areas are mainly located at the bottom area of the map, and these areas require more vehicles to reduce the prevention cost. Therefore, in the solution with the best prevention cost, only fewer vehicles (i.e., fewer separate routes) can be used to meet the travel demand on the top area of the map. This further shows that the travel cost objective and the prevention cost objective conflict with each other.

VI. Conclusion

This paper studies a new VRP4E model under the epidemic scenarios, which considers not only the traditional travel cost objective but also the prevention cost in epidemic situations. As the travel and prevention cost tend to be conflicted with each other, this paper formulates the VRP4E as a multi-objective problem. Furthermore, to solve the VRP4E, this paper proposes the MOACS4E based on the MPMO framework and with two proposed methods, i.e., the PFSG and SQI methods. Extensive experiments and comparisons with state-of-the-art algorithms on 25 benchmark problems and a case study have verified the effectiveness of the proposed MOACS4E.

For future work, the proposed VRP4E model can be further extended with different levels of risks and more other objectives and constraints for various transportation systems in epidemics, such as considering the users' preferred pickup time (period) as a constraint. Furthermore, more kinds of routing, such as hierarchical routing, will be further studied for different situations. In addition, intelligent and efficient techniques from other aspects, e.g., data-driven optimization [63]–[65], knowledge transfer [66], [67], and distributed computation [68]–[70], will be integrated to handle more VRP difficulties in epidemic situations.

References

[1] M. Nishiga, D. W. Wang, Y. Han, D. B. Lewis, and J. C. Wu, "COVID-19 and cardiovascular disease: From basic mechanisms to clinical perspectives," *Nature Rev. Cardiol.*, vol. 17, no. 9, pp. 543–558, Sep. 2020.

[2] (May 2022). *WHO Coronavirus Disease (COVID-19) Dashboard*. [Online]. Available: https://covid19.who.int/

[3] J. H. Kim, F. Marks, and J. D. Clemens, "Looking beyond COVID-19 vaccine phase 3 trials," *Nature Med.*, vol. 27, no. 2, pp. 205–211, Feb. 2021, doi: 10.1038/s41591-021-01230-y.

[4] R. C. Reiner, "Modeling COVID-19 scenarios for the United States," *Nature Med.*, vol. 27, no. 1, pp. 94–105, Jan. 2021.

[5] O. P. Neto *et al.*, "Mathematical model of COVID-19 intervention scenarios for São Paulo—Brazil," *Nature Commun.*, vol. 12, no. 1, pp. 1–13, 2021.

[6] H. Gibbs *et al.*, "Changing travel patterns in China during the early stages of the COVID-19 pandemic," *Nature Commun.*, vol. 11, no. 1, pp. 1–9, 2020.

[7] Q. Xie *et al.*, "COVID-19 patients managed in psychiatric inpatient settings due to first-episode mental disorders in Wuhan, China: Clinical characteristics, treatments, outcomes, and our experiences," *Transl. Psychiatry*, vol. 10, no. 1, pp. 1–11, Dec. 2020.

[8] R. Dhakal *et al.*, "A team effort in nepal: Experiences from managing a large COVID-19 rehabilitation hospital outbreak," *Spinal Cord Ser. Cases*, vol. 7, no. 1, pp. 5–8, Dec. 2021.

[9] X. Yan, H. Huang, Z. Hao, and J. Wang, "A graph-based fuzzy evolutionary algorithm for solving two-echelon vehicle routing problems," *IEEE Trans. Evol. Comput.*, vol. 24, no. 1, pp. 129–141, Feb. 2020.

[10] J. Mandziuk, "New shades of the vehicle routing problem: Emerging problem formulations and computational intelligence solution methods," *IEEE Trans. Emerg. Topics Comput. Intell.*, vol. 3, no. 3, pp. 230–244, Jun. 2019.

[11] K. C. Tan, H. Tang, and S. S. Ge, "On parameter settings of Hopfield networks applied to traveling salesman problems," *IEEE Trans. Circuits Syst. I, Reg. Papers*, vol. 52, no. 5, pp. 994–1002, May 2005.

[12] L. Feng *et al.*, "Explicit evolutionary multitasking for combinatorial optimization: A case study on capacitated vehicle routing problem," *IEEE Trans. Cybern.*, vol. 51, no. 6, pp. 3143–3156, Jun. 2021.

[13] L. Feng *et al.*, "Towards faster vehicle routing by transferring knowledge from customer representation," *IEEE Trans. Intell. Transp. Syst.*, vol. 23, no. 2, pp. 952–965, Feb. 2022, doi: 10.1109/TITS.2020.3018903.

[14] J. Wang, W. Ren, Z. Zhang, H. Huang, and Y. Zhou, "A hybrid multiobjective memetic algorithm for multiobjective periodic vehicle routing problem with time Windows," *IEEE Trans. Syst., Man, Cybern., Syst.*, vol. 50, no. 11, pp. 4732–4745, Nov. 2020.

[15] Y.-N. Guo, J. Cheng, S. Luo, D. Gong, and Y. Xue, "Robust dynamic multi-objective vehicle routing optimization method," *IEEE/ACM Trans. Comput. Biol. Bioinf.*, vol. 15, no. 6, pp. 1891–1903, Nov. 2018.

[16] A. Abdulaal, M. H. Cintuglu, S. Asfour, and O. A. Mohammed, "Solving the multivariant EV routing problem incorporating V2G and G2V options," *IEEE Trans. Transport. Electrific.*, vol. 3, no. 1, pp. 238–248, Mar. 2017.

[17] (Feb. 2021). *Centers for Disease Control and Prevention (CDC)*. [Online]. Available: https://www.cdc.gov/

[18] Z.-H. Zhan, L. Shi, K. C. Tan, and J. Zhang, "A survey on evolutionary computation for complex continuous optimization," *Artif. Intell. Rev.*, vol. 55, no. 1, pp. 59–110, Jan. 2022.

[19] Z.-H. Zhan *et al.*, "Matrix-based evolutionary computation," *IEEE Trans. Emerg. Topics Comput. Intell.*, vol. 6, no. 2, pp. 315–328, Apr. 2022.

[20] J.-Y. Li, Z.-H. Zhan, and J. Zhang, "Evolutionary computation for expensive optimization: A survey," *Mach. Intell. Res.*, vol. 19, no. 1, pp. 3–23, Feb. 2022.

[21] Z.-H. Zhan, J.-Y. Li, and J. Zhang, "Evolutionary deep learning: A survey," *Neurocomputing*, vol. 483, pp. 42–58, Apr. 2022.

[22] M. Dorigo and L. M. Gambardella, "Ant colony system: A cooperative learning approach to the traveling salesman problem," *IEEE Trans. Evol. Comput.*, vol. 1, no. 1, pp. 53–66, Apr. 1997.

[23] T. Liao, K. Socha, M. A. Montes de Oca, T. Stützle, and M. Dorigo, "Ant colony optimization for mixed-variable optimization problems," *IEEE Trans. Evol. Comput.*, vol. 18, no. 4, pp. 503–518, Aug. 2014.

[24] X. Yu, W.-N. Chen, T. Gu, H. Yuan, H. Zhang, and J. Zhang, "ACO-A*: Ant colony optimization plus A* for 3-D traveling in environments with dense obstacles," *IEEE Trans. Evol. Comput.*, vol. 23, no. 4, pp. 617–631, Aug. 2019.

[25] X.-F. Liu, Z.-H. Zhan, J. D. Deng, Y. Li, T. L. Gu, and J. Zhang, "An energy efficient ant colony system for virtual machine placement in cloud computing," *IEEE Trans. Evol. Comput.*, vol. 22, no. 1, pp. 113–128, Feb. 2018.

[26] F. Zheng, A. C. Zecchin, J. P. Newman, H. R. Maier, and G. C. Dandy, "An adaptive convergence-trajectory controlled ant colony optimization algorithm with application to water distribution system design problems," *IEEE Trans. Evol. Comput.*, vol. 21, no. 5, pp. 773–791, Oct. 2017.

[27] S.-Z. Zhou, Z.-H. Zhan, Z.-G. Chen, S. Kwong, and J. Zhang, "A multi-objective ant colony system algorithm for airline crew rostering problem with fairness and satisfaction," *IEEE Trans. Intell. Transp. Syst.*, vol. 22, no. 11, pp. 6784–6798, Nov. 2021.

[28] D. Liang, Z.-H. Zhan, Y. Zhang, and J. Zhang, "An efficient ant colony system approach for new energy vehicle dispatch problem," *IEEE Trans. Intell. Transp. Syst.*, vol. 21, no. 11, pp. 4784–4797, Nov. 2020.

[29] X. Wang, T.-M. Choi, H. Liu, and X. Yue, "Novel ant colony optimization methods for simplifying solution construction in vehicle routing problems," *IEEE Trans. Intell. Transp. Syst.*, vol. 17, no. 11, pp. 3132–3141, Nov. 2016.

[30] L. Shi, Z.-H. Zhan, D. Liang, and J. Zhang, "Memory-based ant colony system approach for multi-source data associated dynamic electric vehicle dispatch optimization," *IEEE Trans. Intell. Transp. Syst.*, early access, Mar. 8, 2022, doi: 10.1109/TITS.2022.3150471.

[31] L.-J. Wu, L. Shi, Z.-H. Zhan, K.-K. Lai, and J. Zhang, "A buffer-based ant colony system approach for dynamic cold chain logistics scheduling," *IEEE Trans. Emerg. Topics Comput. Intell.*, early acces, May 19, 2022, doi: 10.1109/TETCI.2022.3170520.

[32] R. Wang *et al.*, "An adaptive ant colony system based on variable range receding horizon control for berth allocation problem," *IEEE Trans. Intell. Transp. Syst.*, early access, May 18, 2022, doi: 10.1109/TITS.2022.3172719.

[33] Z.-H. Zhan, J. Li, J. Cao, J. Zhang, H. S.-H. Chung, and Y.-H. Shi, "Multiple populations for multiple objectives: A coevolutionary technique for solving multiobjective optimization problems," *IEEE Trans. Cybern.*, vol. 43, no. 2, pp. 445–463, Apr. 2013.

[34] Z.-G. Chen *et al.*, "Multiobjective cloud workflow scheduling: A multiple populations ant colony system approach," *IEEE Trans. Cybern.*, vol. 49, no. 8, pp. 2912–2926, Aug. 2019.

[35] Y. R. Naidu and A. K. Ojha, "Solving multiobjective optimization problems using hybrid cooperative invasive weed optimization with multiple populations," *IEEE Trans. Syst., Man, Cybern., Syst.*, vol. 48, no. 6, pp. 821–832, Jun. 2018.

[36] X.-F. Liu, Z.-H. Zhan, Y. Gao, J. Zhang, S. Kwong, and J. Zhang, "Coevolutionary particle swarm optimization with bottleneck objective learning strategy for many-objective optimization," *IEEE Trans. Evol. Comput.*, vol. 23, no. 4, pp. 587–602, Aug. 2019.

[37] E. Eren and U. R. Tuzkaya, "Safe distance-based vehicle routing problem: Medical waste collection case study in COVID-19 pandemic," *Comput. Ind. Eng.*, vol. 157, Jul. 2021, Art. no. 107328.

[38] E. B. Tirkolaee, P. Abbasian, and G. W. Weber, "Sustainable fuzzy multi-trip location-routing problem for medical waste management during the COVID-19 outbreak," *Sci. Total Environ.*, vol. 756, Feb. 2021, Art. no. 143607.

[39] J. Pacheco and M. Laguna, "Vehicle routing for the urgent delivery of face shields during the COVID-19 pandemic," *J. Heuristics*, vol. 26, no. 5, pp. 619–635, Aug. 2020.

[40] K. Lin and S. N. Musa, "Vehicle routing optimization for pandemic containment: A systematic review on applications and solution approaches," *Sustainability*, vol. 14, pp. 1–27, Feb. 2022.

[41] F. Majzoubi, L. Bai, and S. S. Heragu, "The EMS vehicle patient transportation problem during a demand surge," *J. Global Optim.*, vol. 79, no. 4, pp. 989–1006, Apr. 2021.

[42] M.-X. Zhang, H.-F. Yan, J.-Y. Wu, and Y.-J. Zheng, "Quarantine vehicle scheduling for transferring high-risk individuals in epidemic areas," *Int. J. Environ. Res. Public Health*, vol. 17, no. 7, p. 2275, Mar. 2020.

[43] M. Mook, E. Kloth, and J. Lee, "Isolation and quarantine policy for connected vehicles routing," in *Proc. IISE Annu. Conf. Expo.*, 2019, pp. 1590–1596.

[44] Y.-L. Tsai, C. Rastogi, P. K. Kitanidis, and C. B. Field, "Routing algorithms as tools for integrating social distancing with emergency evacuation," *Sci. Rep.*, vol. 11, no. 1, pp. 1–14, Dec. 2021.

[45] Y. Jiang, B. Bian, and Y. Liu, "Integrated multi-item packaging and vehicle routing with split delivery problem for fresh agri-product emergency supply at large-scale epidemic disease context," *J. Traffic Transp. Eng.*, vol. 8, no. 2, pp. 196–208, Apr. 2021.

[46] T. Zhao *et al.*, "Optimizing living material delivery during the COVID-19 outbreak," *IEEE Trans. Intell. Transp. Syst.*, early access, Mar. 17, 2021, doi: 10.1109/TITS.2021.3061076.

[47] B. Y. Qu, Y. S. Zhu, Y. C. Jiao, M. Y. Wu, P. N. Suganthan, and J. J. Liang, "A survey on multi-objective evolutionary algorithms for the solution of the environmental/economic dispatch problems," *Swarm Evol. Comput.*, vol. 38, no. 1, pp. 1–11, Feb. 2018.

[48] Y. Wang, J. Chen, and Y. Shen, "A multi-objective optimization model for VRP and VFP based on an improved ant colony algorithm," in *Proc. IEEE 3rd Adv. Inf. Manage., Communicates, Electron. Autom. Control Conf. (IMCEC)*, Oct. 2019, pp. 777–780.

[49] V. N. Kubil, V. A. Mokhov, and D. V. Grinchenkov, "Multi-objective ant colony optimization for multi-depot heterogenous vehicle routing problem," in *Proc. Int. Conf. Ind. Eng., Appl. Manuf. (ICIEAM)*, May 2018, pp. 1–6.

[50] M. Liu, X. You, X. Yu, and S. Liu, "KL divergence-based pheromone fusion for heterogeneous multi-colony ant optimization," *IEEE Access*, vol. 7, pp. 152646–152657, 2019.

[51] H. Zhu, X. You, and S. Liu, "Multiple ant colony optimization based on Pearson correlation coefficient," *IEEE Access*, vol. 7, pp. 61628–61638, 2019.

[52] J. Li. (Apr. 21, 2022). *JD.com's 'Suicide Logistics' Goes to Shanghai to Sleep on the Road for People who are Blocked | Aid | Neighborhood Committee*. Epoch Times. [Online]. Available: https://www.breakinglatest.news/news/jd-coms-suicide-logistics-goes-to-shanghai-to-sleep-on-the-road-for-people-who-are-blocked-aid-neighborhood-committee/

[53] G. A. Croes, "A method for solving traveling-salesman problems," *Oper. Res.*, vol. 6, no. 6, pp. 791–812, Dec. 1958.

[54] S.-H. Wu, Z.-H. Zhan, and J. Zhang, "SAFE: Scale-adaptive fitness evaluation method for expensive optimization problems," *IEEE Trans. Evol. Comput.*, vol. 25, no. 3, pp. 478–491, Jun. 2021.

[55] E. Zitzler and L. Thiele, "Multiobjective evolutionary algorithms: A comparative case study and the strength Pareto approach," *IEEE Trans. Evol. Comput.*, vol. 3, no. 4, pp. 257–271, Nov. 1999.

[56] K. Deb, A. Pratap, S. Agarwal, and T. Meyarivan, "A fast and elitist multiobjective genetic algorithm: NSGA-II," *IEEE Trans. Evol. Comput.*, vol. 6, no. 2, pp. 182–197, Jan. 2002.

[57] Q. Zhang and H. Li, "MOEA/D: A multiobjective evolutionary algorithm based on decomposition," *IEEE Trans. Evol. Comput.*, vol. 11, no. 6, pp. 712–731, Dec. 2007.

[58] J. Wang, T. Weng, and Q. Zhang, "A two-stage multiobjective evolutionary algorithm for multiobjective multidepot vehicle routing problem with time windows," *IEEE Trans. Cybern.*, vol. 49, no. 7, pp. 2467–2478, Jul. 2019.

[59] Y. Tian, T. Zhang, J. Xiao, X. Zhang, and Y. Jin, "A coevolutionary framework for constrained multiobjective optimization problems," *IEEE Trans. Evol. Comput.*, vol. 25, no. 1, pp. 102–116, Feb. 2021.

[60] Z. Zhang, H. Qin, and Y. Li, "Multi-objective optimization for the vehicle routing problem with outsourcing and profit balancing," *IEEE Trans. Intell. Transp. Syst.*, vol. 21, no. 5, pp. 1987–2001, May 2020.

[61] (Mar. 2022). *COVID-19 Prevention and Control Plan (7th Edition)*. [Online]. Available: http://www.gov.cn/xinwen/2020-09/15/5543680/files/931ddbb00e134025bbb86739c8ed68ee.pdf

[62] (Mar. 2022). *Data of 199 County-Level Regions in AMAP*. [Online]. Available: https://maplab.amap.com/share/mapv/bc30a135f5d2a493d02ed5d2c171cf0d

[63] J.-Y. Li, Z.-H. Zhan, C. Wang, H. Jin, and J. Zhang, "Boosting data-driven evolutionary algorithm with localized data generation," *IEEE Trans. Evol. Comput.*, vol. 24, no. 5, pp. 923–937, Oct. 2020.

[64] J.-Y. Li, Z.-H. Zhan, H. Wang, and J. Zhang, "Data-driven evolutionary algorithm with perturbation-based ensemble surrogates," *IEEE Trans. Cybern.*, vol. 51, no. 8, pp. 3925–3937, Aug. 2021.

[65] J.-Y. Li, Z.-H. Zhan, J. Xu, S. Kwong, and J. Zhang, "Surrogate-assisted hybrid-model estimation of distribution algorithm for mixed-variable hyperparameters optimization in convolutional neural networks," *IEEE Trans. Neural Netw. Learn. Syst.*, early access, Sep. 20, 2021, doi: 10.1109/TNNLS.2021.3106399.

[66] J.-Y. Li, Z.-H. Zhan, K. C. Tan, and J. Zhang, "A meta-knowledge transfer-based differential evolution for multitask optimization," *IEEE Trans. Evol. Comput.*, early access, Nov. 29, 2021, doi: 10.1109/TEVC.2021.3131236.
[67] S.-H. Wu, Z.-H. Zhan, K. C. Tan, and J. Zhang, "Orthogonal transfer for multitask optimization," *IEEE Trans. Evol. Comput.*, early access, Mar. 17, 2022, doi: 10.1109/TEVC.2022.3160196.
[68] J.-Y. Li, K.-J. Du, Z.-H. Zhan, H. Wang, and J. Zhang, "Distributed differential evolution with adaptive resource allocation," *IEEE Trans. Cybern.*, early access, Mar. 14, 2022, doi: 10.1109/TCYB.2022.3153964.
[69] J.-Y. Li, Z.-H. Zhan, R.-D. Liu, C. Wang, S. Kwong, and J. Zhang, "Generation-level parallelism for evolutionary computation: A pipeline-based parallel particle swarm optimization," *IEEE Trans. Cybern.*, vol. 51, no. 10, pp. 4848–4859, Oct. 2021.
[70] J.-Y. Li, Z.-H. Zhan, K. C. Tan, and J. Zhang, "Dual differential grouping: A more general decomposition method for large-scale optimization," *IEEE Trans. Cybern.*, early access, Mar. 25, 2022, doi: 10.1109/TCYB.2022.3158391.

Jian-Yu Li (Student Member, IEEE) received the B.S. degree in computer science and technology from the South China University of Technology, Guangzhou, China, in 2018, where he is currently pursuing the Ph.D. degree in computer science and technology with the School of Computer Science and Engineering. His research interests mainly include computational intelligence; data-driven optimization; machine learning, including deep learning, and their applications in real-world problems; and in environments of distributed computing and big data. He has been invited as a Reviewer of the IEEE TRANSACTIONS ON EVOLUTIONARY COMPUTATION and the *Neurocomputing* journal, and the Program Community Member and a reviewer of some international conferences.

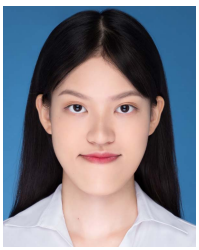

Xin-Yi Deng is currently pursuing the B.S. degree in Chinese language and literature (teacher education) with the School of Chinese Language and Literature, South China Normal University, Guangzhou, China. Her research interests mainly include language, literature, and computational intelligence.

Zhi-Hui Zhan (Senior Member, IEEE) received the bachelor's and Ph.D. degrees in computer science from Sun Yat-sen University, Guangzhou, China, in 2007 and 2013, respectively. He is currently the Changjiang Scholar Young Professor with the School of Computer Science and Engineering, South China University of Technology, Guangzhou. His current research interests include evolutionary computation, swarm intelligence, and their applications in real-world problems and in environments of cloud computing and big data. He was the recipient of the IEEE Computational Intelligence Society (CIS) Outstanding Early Career Award in 2021, the Outstanding Youth Science Foundation from National Natural Science Foundations of China (NSFC) in 2018, and the Wu Wen-Jun Artificial Intelligence Excellent Youth from the Chinese Association for Artificial Intelligence in 2017. His doctoral dissertation was awarded the IEEE CIS Outstanding Ph.D. Dissertation and the China Computer Federation Outstanding Ph.D. Dissertation. He is one of the World's Top 2% Scientists for both Career-Long Impact and Year Impact in artificial intelligence and one of the Highly Cited Chinese Researchers in computer science. He is currently the Chair of the Membership Development Committee in IEEE Guangzhou Section and the Vice-Chair of the IEEE CIS Guangzhou Chapter. He is currently an Associate Editor of the IEEE TRANSACTIONS ON EVOLUTIONARY COMPUTATION, the *Neurocomputing*, and the *Memetic Computing*.

Liang Yu received the Ph.D. degree in photogrammetry and remote sensing from Wuhan University in 2008. He is currently the Director of data science in smart transportation with Alibaba Cloud. Prior to Alibaba, he did postdoctoral research with the National University of Singapore, the National Center for Supercomputing Applications of the University of Illinois at Urbana-Champaign, and Singapore-MIT Alliance for Research and Technology. He had been leading the Smart Mobility Group, Institute of Infocomm Research, Singapore, where he initiated many research efforts to transportation and urban planning. His research interest has covered a wide range of smart city topics such as geospatial data integration, data semantics, and data analytics.

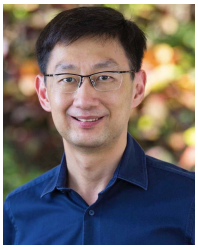

Kay Chen Tan (Fellow, IEEE) received the B.Eng. degree (Hons.) and the Ph.D. degree from the University of Glasgow, U.K., in 1994 and 1997, respectively. He is currently the Chair Professor (computational intelligence) with the Department of Computing, The Hong Kong Polytechnic University. He has published over 300 refereed articles and seven books. He is currently the Vice-President (Publications) of IEEE Computational Intelligence Society, USA. He currently serves as an Editorial Board Member for more than ten journals. He served as the Editor-in-Chief for the *IEEE Computational Intelligence Magazine* from 2010 to 2013 and the IEEE TRANSACTIONS ON EVOLUTIONARY COMPUTATION from 2015 to 2020. He is an IEEE Distinguished Lecturer Program (DLP) Speaker and the Chief Co-Editor of *Machine Learning: Foundations, Methodologies, and Applications* (Springer) book series.

Kuei-Kuei Lai received the Ph.D. degree in management science from Tamkang University, Taiwan. He is currently a Professor with the Department of Business Administration, Chaoyang University of Technology, Taiwan. He is the author of more than 90 articles. His research interests include quantitative analysis, patent citation analysis, social networks analysis, technology strategy and technological forecasting, computational intelligence, and applications in management.

Jun Zhang (Fellow, IEEE) received the Ph.D. degree from the City University of Hong Kong, Hong Kong, in 2002. He is currently a Korea Brain Pool Fellow Professor with Hanyang University, South Korea. His current research interests include computational intelligence, cloud computing, operations research, and power electronic circuits. He has published over more than 150 IEEE TRANSACTIONS papers in his research areas. He was a recipient of the Changjiang Chair Professor from the Ministry of Education, China, in 2013; the National Science Fund for Distinguished Young Scholars of China in 2011; and the First-Grade Award in Natural Science Research from the Ministry of Education, China, in 2009. He is currently an Associate Editor of the IEEE TRANSACTIONS ON EVOLUTIONARY COMPUTATION and the IEEE TRANSACTIONS ON CYBERNETICS.